Crystallization process and some properties of novel transparent machinable calcium-mica glass-ceramics

Seiichi Taruta *, Michita Sakata, Tomohiro Yamaguchi, Kunio Kitajima

*Department of Chemistry and Materials Engineering, Faculty of Engineering, Shinshu University,
4-17-1 Wakasato, Nagano-shi, Nagano 380-8553, Japan*

Abstract

Bulk glass having a calcium-mica composition ($Ca_{0.5}Mg_3AlSi_3O_{10}F_2$) is homogeneous glass. The crystallization mechanism of the mica is surface crystallization and transparency is lost completely when crystallization occurs on the surface. In this study, by decreasing SiO_2 and increasing CaO and Al_2O_3 from the chemical composition of $Ca_{0.5}Mg_3AlSi_3O_{10}F_2$, and moreover by replacing a small amount of K_2O instead of CaO, the phase separation appears in the glasses. Because of this phase separation, the mica begins to be crystallized not only on the surface but also in the bulk at lower temperatures. Consequently, the novel transparent machinable mica glass-ceramic can be obtained by heating the glasses having the chemical composition of $Ca_{0.6}Mg_3Al_{1.2}Si_{2.8}O_{10}F_2$ and $K_{0.01}Ca_{0.595}Mg_3Al_{1.2}Si_{2.8}O_{10}F_2$. As a larger amount of calcium-mica is separated, the bending strength decreases and the fracture toughness increases. Furthermore, by replacing K^+ ion instead of Ca^{2+} ion in the interlayer of calcium-mica, the interlayer bonding strength becomes high, resulting in the increase of the bending strength.
© 2006 Elsevier Ltd and Techna Group S.r.l. All rights reserved.

Keywords: B. Microstructure-final; C. Mechanical properties; D. Glass ceramics

1. Introduction

Mica glass-ceramics are the typical machinable ceramics. The machinability originates in the cleavage of mica crystals and the interlocking structure formed by the flake-like mica crystals. The structural formula of the mica is generally expressed as $X_{0.5-1}Y_{2-3}Z_4O_{10}(OH,F)_2$, where X, Y and Z are cations in 12-, 6- and 4-fold coordination, and extensive solid solutions are possible. For the representative commercial mica-type glass-ceramic, MACOR® and DICOR®, the micas are phlogopite-type ($K_{1-x}Mg_3Al_{1-x}Si_{3+x}O_{10}F_2$) and tetrasilicic type ($K_{1-x}Mg_{2.5+x/2}Si_4O_{10}F_2$), respectively, and their interlayer cations, that is, X, are K^+ ions [1]. The glass-ceramics consisting of phlogopite-type mica, in which K^+ ion is replaced by alkaline earth ions such as Ca^{2+}, Sr^{2+} and Ba^{2+} ions, are known as alkaline earth mica glass-ceramics [2]. Among these, the calcium-mica glass-ceramic has the greatest glass stability of the melt [2]. Therefore, the large bulk glass having a calcium-mica composition ($Ca_{0.5}Mg_3AlSi_3O_{10}F_2$) is easily prepared by the

melting method. Conversely, natural micas consisting of interlayer cations of alkaline earth ions, brittle micas, are distinguished from true micas by a layer charge per formula unit of approximately -2.0 [3]. For example, clintonite ($Ca(Mg_2Al)(SiAl_3)O_{10}(OH)_2$), margarite ($CaAl_2(Si_2Al_2)O_{10}(OH)_2$) and kinoshitalite ($BaMg_3(Si_2Al_2)O_{10}(OH)_2$), are known as brittle micas [3]. In addition, highly charged sodium fluorophlogopite mica ($Na_4Mg_6Al_4Si_4O_{20}F_4$), called "Na-4-mica", has been synthesized by many kinds of solid-state reactions [4–14]. Also, it has been found that electrical conductivity of the "Na-4-mica" is 4.3×10^{-4} S/cm at 650 °C, which is much higher than that of the ordinary Na-type fluorophlogopite ($Na_2Mg_6Al_2Si_6O_{20}F_4$) [14]. Consequently, if the glass-ceramic consisting of highly charged calcium fluorophlogopite mica ($CaMg_3Al_2Si_2O_{10}F_2$) is prepared, its electrical conductivity is much higher than that of ordinary calcium-mica glass-ceramic.

In this study, preparation of parent glasses having the chemical composition of $Ca_xMg_3Al_{2x}Si_{(4-2x)}O_{10}F_2$ ($x = 0.5–1.0$) was attempted. While bulk glasses with $x \geq 0.7$ prepared by the ordinary melting method are devitrified, novel transparent machinable glass-ceramic was obtained from the parent glass with $x = 0.6$. Subsequently, the crystallization process of the parent glass with $x = 0.6$ and some properties such as mechanical

* Corresponding author. Tel.: +81 26 269 5416; fax: +81 26 269 5424.
E-mail address: staruta@shinshu-u.ac.jp (S. Taruta).

strength, electrical conductivity, etc. of the obtained glass-ceramics were investigated. In addition, a small amount of CaO in the parent glass with $x = 0.6$ was replaced by K_2O and the crystallization process and its properties were also investigated. Introduction of K^+ ion into the interlayer of calcium-mica was used to prevent water-swelling which is a feature of calcium-mica and a fatal demerit of the glass-ceramics.

2. Experimental procedure

The reagents of MgO, Al_2O_3, SiO_2, K_2CO_3, $CaCO_3$ and MgF_2 were mixed in the chemical composition corresponding to $Ca_{0.6}Mg_3Al_{1.2}Si_{2.8}O_{10}F_2$ or $K_{0.01}Ca_{0.595}Mg_3Al_{1.2}Si_{2.8}O_{10}F_2$. The mixtures were calcined at 900 °C for 1 h, melted in a sealed platinum container at 1450 °C for 2 h, and then cooled outside of the furnace. The obtained glasses were then annealed at ~20 °C higher temperatures than their glass-transition temperatures, and cooled at 2 °C/min to eliminate strain. It was confirmed by X-ray diffraction (XRD) analysis that the parent

glasses prepared by such a method were not devitrified. The parent glasses were then heated at 750–1000 °C at a heating rate of 10 °C/min for 2 h to crystallize them. As a reference, the calcium-mica glass-ceramic having the chemical composition of $Ca_{0.5}Mg_3AlSi_3O_{10}F_2$ was prepared by the same method. The three specimens having the chemical composition of $Ca_{0.5}Mg_3AlSi_3O_{10}F_2$, $Ca_{0.6}Mg_3Al_{1.2}Si_{2.8}O_{10}F_2$ or $K_{0.01}Ca_{0.595}Mg_3Al_{1.2}Si_{2.8}O_{10}F_2$ are shown as Ca05, Ca06 or CaK001 specimens, respectively, in this paper.

The phase change of the parent glasses was analyzed using XRD, and the microstructure development was observed using a field-emission type scanning electron microscope (FE-SEM). For the observation, the specimens were polished by diamond slurries and chemically etched by 5 mass% hydrofluoric acid.

The three-point bending strength was measured using a universal strength testing machine. The crosshead speed for the bending test was 0.5 mm/min. The hardness and fracture toughness were measured using a Vickers diamond indenter which was indented on the polished surface of specimens at
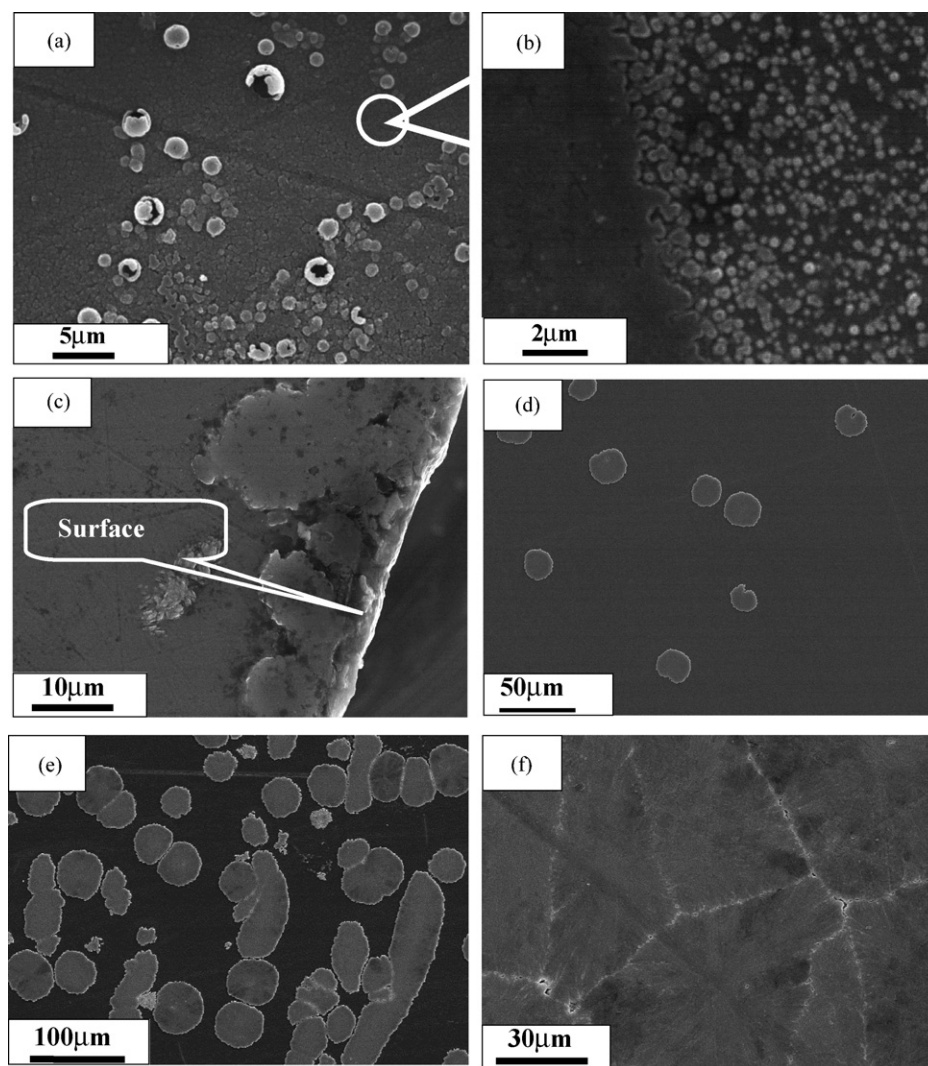

Fig. 1. SEM photographs of polished and chemically etched surfaces of the Ca06 parent glass at (a) low magnification and (b) high magnification, (c) near the surface and (d) deep inside of the Ca06 specimen heated at 770 °C for 2 h, and (e) and (f) deep inside of the Ca06 specimen heated for 2 h at 800 and 850 °C, respectively. The "Surface" shown in the figure is the original surface of the specimen which was not polished.
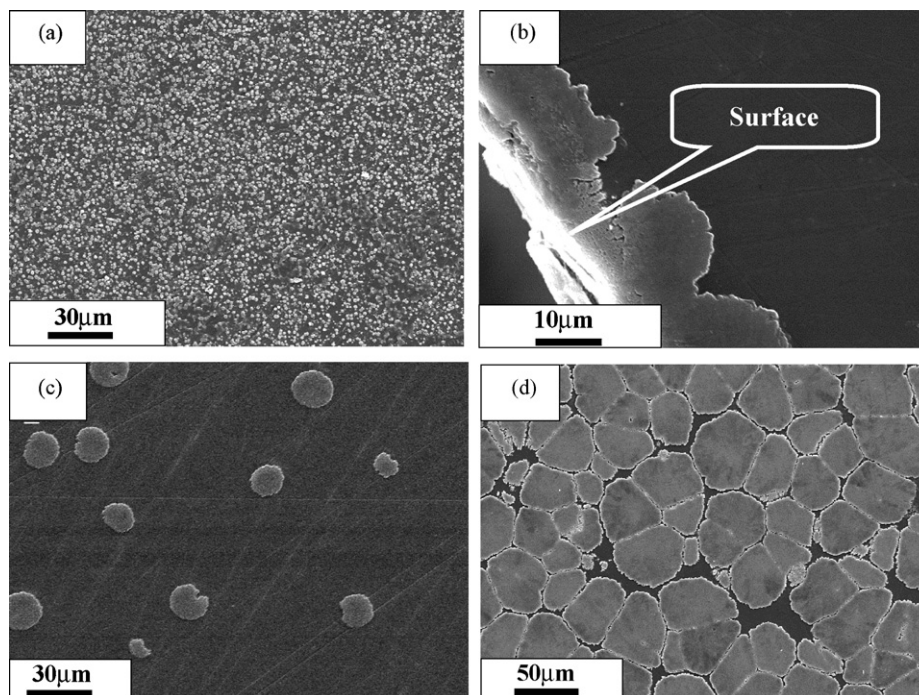
Fig. 2. SEM photographs of polished and chemically etched surfaces of (a) the CaK001 parent glass, (b) near the surface and (c) deep inside of the CaK001 specimen heated at 740 °C for 2 h and (d) deep inside of the CaK001 specimen heated at 780 °C for 2 h. The "Surface" shown in the figure is the original surface of the specimen which was not polished.

load of 98 N for 10 s. The fracture toughness was determined by the indentation microfracture method (IM method). The machinability was qualitatively evaluated using a bench-drilling machine. The drill was conventional high-speed steel and the rotational frequency was 620 rpm. Specific electrical resistance of the specimens was measured at 100–650 °C by the four-probe method using an impedance analyzer in a frequency range of $4–10^6$ Hz.

3. Results and discussion

3.1. Crystallization process

The parent glass having the chemical composition of $Ca_{0.5}Mg_3AlSi_3O_{10}F_2$ is homogeneous glass and does not show a phase separation structure [15]. Mica was first separated near the surface at 775–800 °C, and then grew radially [15]. It is clear that the crystallization mechanism of this specimen was surface crystallization.

The SEM photographs of the polished and chemically etched surface of the Ca06 parent glass and the heated Ca06 specimen are shown in Fig. 1. In the parent glass, a large droplet phase with a size of 0.5–2.0 μm (Fig. 1(a)) and a fine droplet-like phase with a size of <0.5 μm were observed. The spherical phase with a size of 10–20 μm first appeared not only near the surface but also inside of the specimen heated at 770 °C, though crystals were not detected by XRD analysis. The spherical phase observed near the surface in Fig. 1(c) was mica separated on and near the original surface of the specimen. The spherical phases observed in Fig. 1(d) were mica separated inside of the specimen, but were not mica grown from the original surface.

Mica was detected in the specimen heated at ≥780 °C by XRD analysis. As the heating temperature increased, the spherical phases of mica grew radially and impinged upon one another as shown in Fig. 1(e). At 850 °C, cellular membrane-like microstructure of mica was observed all over the specimen.

The SEM photographs of the polished and chemically etched surface of the CaK001 parent glass and the heated CaK001 specimen are shown in Fig. 2. In the CaK001 parent glass, a droplet phase with a size of 0.5 μm (Fig. 2(a)) was observed. The mica was first separated at 740 °C. It appeared not only near the surface but also inside of the specimen, and grew radially as did the mica in the Ca06 specimen. The crystal phase that separated in the Ca05, Ca06 and CaK001 specimens heated at ≤1000 °C was only mica.

The basal spacing ($c \sin \beta$; c and β are lattice constants) and lattice constant b of the mica separated in the heat treated Ca05, Ca06 and CaK001 specimens were measured, and found to be independent of the heating temperature. The obtained basal spacing and lattice constant b are shown in Fig. 3. In addition, the reported basal spacing and lattice constant b of trisilicic type micas [2,16,17], tetrasilicic type micas [18–20] and brittle mica (kinoshitalite) [21] are plotted as a reference in the Fig. 3. In general, the basal spacing, which is the distance between basal planes in the vertical direction relative to the layer, depends mainly on the size of interlayer ion and the electrostatic repulsion between layers. Furthermore, the lattice constant b is a standard for determining whether the mica is tetrasilicic type or trisilicic type, and the b of tetrasilicic type mica is shown to be smaller than that of trisilicic type mica. Based on this point, Ca-phlogopite [16] shown as a reference in Fig. 3 is not trisilicic type mica (phlogopite) but may be
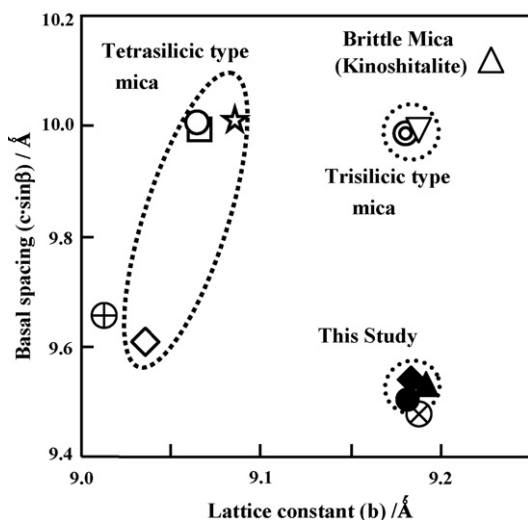
Fig. 3. Relationship between basal spacing ($c \sin \beta$) and lattice constant (b) of mica crystals showing: (●) Ca05, (▲) Ca06 and (◆) CaK001 specimens. Trisilicic type micas: (▽ [16], ⊙ [17]) K-phlogopite ($KMg_3(AlSi_3O_{10})F_2$) and (⊕ [16], ⊗ [2]) Ca-phlogopite ($Ca_{0.5}Mg_3(AlSi_3O_{10})F_2$). Tetrasilicic type micas: (○ [18], □ [19]) K-taeniolite ($KMg_2Li(Si_4O_{10})F_2$), (◇ [18]) Na-taeniolite ($NaMg_2Li(Si_4O_{10})F_2$) and (☆ [20]) K-tetrasilicic mica ($KMg_{2.5}(Si_4O_{10})F_2$). Brittle mica: (△ [21]) kinoshitalite ($BaMg_3(Al_2Si_2O_{10})F_2$).

tetrasilicic type mica. In addition, the b of kinoshitalite is larger than that of trisilicic type micas because a larger amount of the Al^{3+} ion, which is larger cation than the Si^{4+} ion, is placed in the four-fold coordination sites of kinoshitalite. The b and $c \sin \beta$ of micas separated in the Ca05, Ca06 and CaK001 specimens were close to those of Ca-phlogopite in the glass-ceramic prepared by Hoda and Beall [2]. Moreover, the b values were close to those of trisilicic type mica. That is, the micas in the Ca05, Ca06 and CaK001 specimens corresponded to Ca-phlogopite. However, the b and $c \sin \beta$ of mica in the Ca06 specimen were slightly larger than those of mica in the Ca05 specimen meaning that the mica in the Ca06 specimen had a larger amount of Al^{3+} ion in the four-fold coordination sites and a larger amount of the Ca^{2+} ion in the interlayer as compared with the mica in the Ca05 specimen. That is, the mica in the Ca06 specimen was a little closer to the characteristic of brittle micas. The b of mica in the CaK001 specimen was a little smaller than that of mica in the Ca06 specimen but the $c \sin \beta$ was a little larger suggesting that the K^+ ion replaced the Ca^{2+} ion in the interlayer and the mica went back to trisilicic type mica.
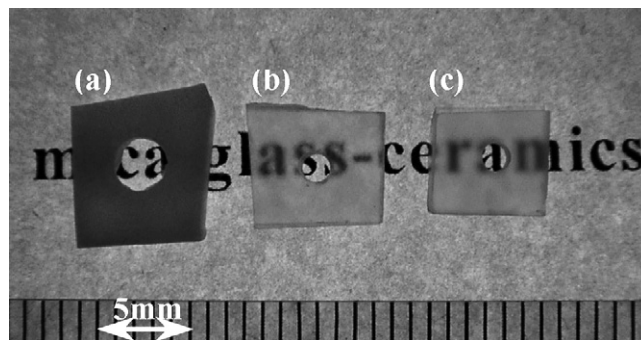

Fig. 4. Photograph of drilling test for (a) Ca05 specimen heated at 850 °C, (b) Ca06 specimen heated at 800 °C and (c) CaK001 specimen heated at 780 °C for 2 h.

3.2. Some properties

The photographs of the drilling test for the heated Ca05, Ca06 and CaK001 specimens with thickness of about 2 mm are shown in Fig. 4. It is clear from this figure that the Ca06 and CaK001 specimens were transparent even though the mica was separated. The Ca05 specimen heated at 850 °C and the transparent CaK001 specimen heated at 780 °C were easily machined because the mica crystals formed the interlocking microstructure. Though the transparent Ca06 specimen heated at 800 °C could be machined, it took the drill more time to penetrate into the specimen. In the transparent Ca06 specimen, the mica crystal phase was not separated all over the specimen as shown in Fig. 1(e), and it might have been formed as a loose continuous phase.

Some properties of the heated Ca05, Ca06 and CaK001 specimens are shown in Table 1. The bending strength of the Ca06 specimen became lower because a larger amount of the calcium-mica, which has a low interlayer bonding strength, was separated. By replacing the K^+ ion instead of the Ca^{2+} ion in the interlayer, the interlayer bonding strength becomes higher. Therefore, the bending strength of the CaK001 specimen was higher than that of the Ca06 specimen. The fracture toughness became higher because a larger amount of mica was separated. While the bending strength of the transparent machinable CaK001 specimen was lower than that of the translucent Dicor® glass-ceramic, the fracture toughness was higher. The electrical conductivity of the Ca06 specimen became higher because a larger amount of mica was separated. The Ca06 specimen heated at 850 °C showed

Table 1
The properties of obtained glass-ceramics and Dicor® glass-ceramic

Specimen	Heating condition	Bending strength (MPa)	Hardness (GPa)	Fracture toughness (MPa m$^{0.5}$)	Electrical conductivity at 650 °C (S/cm)	Water resistance
Ca05	850 °C, 2 h				3.9×10^{-7}	×
Ca06	800 °C, 2 h	94 ± 13	5.4 ± 0.5	1.1 ± 0.2	3.6×10^{-7}	○
	850 °C, 2 h	86 ± 5	4.0 ± 1.3	2.8 ± 0	4.5×10^{-7}	×
CaK001	780 °C, 2 h	114 ± 15	3.7 ± 0.5	1.7 ± 0		○
Dicor® code 9670 [1]		138	3.3	1.5		

(×) The specimen was disintegrated by the water-swelling of mica in water; (○) the appearance of the specimen was not changed in water.

higher electrical conductivity than the Ca05 specimen heated at 850 °C even though a larger amount of mica was separated in the both specimens. These results suggest that the conductivity species was the Ca^{2+} ion and the main conductivity path was the interlayer of mica, and the introduction of a large number of cations in the interlayer of mica will cause higher electrical conductivity. The Ca05 and Ca06 specimen in which a large amount of mica was separated were disintegrated in the water by the water-swelling of calcium-mica. However, the Ca06 specimen heated at 800 °C, with the mica forming loose interlocking structure, was not disintegrated in the water even after 3 months. The water resistance of the CaK001 specimen heated at 780 °C shows that the introduction of a small amount of K^+ ion in the interlayer of the calcium-mica prevented the water-swelling of calcium-mica.

4. Conclusions

The bulk glass having a calcium-mica composition $(Ca_{0.5}Mg_3AlSi_3O_{10}F_2)$ was homogeneous, and the crystallization mechanism of the mica was surface crystallization. The transparency was lost completely when crystallization occurred on the surface. By decreasing SiO_2 and increasing CaO and Al_2O_3 from the chemical composition of $Ca_{0.5}Mg_3AlSi_3O_{10}F_2$, the phase separation consisting of two droplet and matrix phases appeared in the glass. Additionally, due to the phase separation, the mica was separated not only on the surface but also in the bulk at lower temperatures. Furthermore, by replacing a small amount of K_2O instead of CaO in the chemical composition of $Ca_{0.6}Mg_3Al_{1.2}Si_{2.8}O_{10}F_2$, the phase separation consisting of one droplet and matrix phases appeared in the glass and mica was separated not only on the surface but also in the bulk at still lower temperatures. So the novel transparent machinable mica glass-ceramic could be obtained by heating such phase separated glasses, and they were not disintegrated by water-swelling of calcium-mica. As a larger amount of calcium-mica was separated, the bending strength was decreased and the fracture toughness was increased. However, replacing a small amount of K^+ ion instead of Ca^{2+} ion in the interlayer of mica resulted in the increase of the bending strength.

Acknowledgements

References

[1] W. Höland, G. Beall, Glass-Ceramic Technology, The American Ceramic Society, Westerville, OH, 2002.

[2] S.N. Hoda, G.H. Beall, Alkaline earth mica glass-ceramics, in: J.H. Simmous, D.R. Uhlmann, G.H. Beall (Eds.), Advances in Nucleation and Crystallization in Glasses, The American Ceramic Society, Westerville, OH, 1982, pp. 287–300.

[3] S. Guggenheim, The brittle micas, in: S.W. Bailey (Ed.), P.H. Ribbe (Series Ed.), Reviews in Mineralogy, vol.13, Micas, Mineral. Soc. Am., Washington, DC, 1984, pp. 61–104.

[4] M. Gregorkiewitz, J.A. Rausell-Colom, Characterization and properties of a new synthetic silicate with highly charged mica-type layers, Am. Mineral. 72 (1987) 515–527.

[5] W.J. Paulus, S. Komarneni, R. Roy, Bulk synthesis and selective exchange of strontium ions in $Na_4Mg_6Al_4Si_4O_{20}F_4$ mica, Nature 357 (1992) 571–573.

[6] K.R. Franklin, E. Lee, Synthesis and ion-exchange properties of Na-4-mica, J. Mater. Chem. 6 (1996) 109–115.

[7] S. Komarneni, R. Pidugu, J.E. Amonette, Synthesis of Na-4-mica from metakaolinite and MgO: characterization and Sr^{2+} uptake kinetics, J. Mater. Chem. 8 (1998) 205–208.

[8] T. Kodama, S. Komarneni, Alkali metal and alkaline earth metal ion exchange with Na-4-mica prepared by a new synthetic route from kaolinite, J. Mater. Chem. 9 (1999) 2475–2480.

[9] S. Komarneni, R. Pidugu, W. Hoffbauer, H. Schneider, A synthetic Na-rich mica: synthesis and characterization by ^{27}Al and ^{29}Si magic angle spinning nuclear magnetic resonance spectroscopy, Crays Clay Miner. 47 (1999) 410–416.

[10] T. Kodama, S. Komarneni, W. Hoffbauer, H. Schneider, Na-4-mica: simplified synthesis from kaolinite, characterization and Zn, Cd, Pb, Cu and Ba uptake kinetics, J. Mater. Chem. 10 (2000) 1649–1653.

[11] T. Kodama, Y. Harada, M. Ueda, K. Shimizu, K. Shuto, S. Komarneni, W. Hoffbauer, H. Schneider, Crystal-size control and characterization of Na-4-mica prepared from kaolinite, J. Mater. Chem. 11 (2001) 1222–1227.

[12] M. Park, D.H. Lee, C.L. Choi, S.S. Kim, K.S. Kim, J. Choi, Pure Na-4-mica: synthesis and characterization, Chem. Mater. 14 (2002) 2582–2589.

[13] T. Kodama, M. Ueda, Y. Nakamuro, K. Shimizu, S. Komarneni, Ultrafine Na-4-mica: uptake of alkali and alkaline earth metal cations by ion exchange, Langmuir 20 (2004) 4920–4925.

[14] S. Taruta, S. Shimodaira, T. Yamaguchi, K. Kitajima, New synthetic method and ionic conductivity of Na-4-mica, Mater. Lett. 60 (2006) 464–466.

[15] S. Taruta, K. Mukoyama, S.S. Suzuki, K. Kitajima, N. Takusagawa, Crystallization process and some properties of calcium mica-apatite glass-ceramics, J. Non-Cryst. Solids 296 (2001) 201–211.

[16] S. Lyng, J. Markali, J. Krogh-Moe, N.H. Lundberg, On the crystallization in aluminosilicate glasses containing fluoride and magnesia, Phys. Chem. Glasses 11 (1970) 6–10.

[17] Card No. 16-344, Joint Committee on Powder Diffraction Standards, Swarthmore, PA.

[18] K. Kitajima, S. Taruta, N. Takusagawa, Effect of layer charge on the IR spectra of synthetic fluorine micas, Clay Miner. 26 (1991) 435–440.

[19] H. Toraya, S. Iwai, F. Marumo, M. Hirao, The crystal structure of taeniolite, $KLiMg_2Si_4O_{10}F_2$, Z. Kristallogr. 146 (1977) 73–83.

[20] H. Toraya, S. Iwai, F. Marumo, M. Daimon, R. Kondo, The crystal structure of tetrasilicic potassium fluor mica, $KMg_{2.5}Si_4O_{10}F_2$, Z. Kristallogr. 144 (1976) 42–52.

[21] Card No. 29-181, Joint Committee on Powder Diffraction Standards, Swarthmore, PA.